DMD Fast Forward. Published on February 6, 2008 as doi:10.1124/dmd.107.018960
This article has not been copyedited and formatted. The final version may differ from this version.

DMD 18960

CYP1B1 IS NOT A MAJOR DETERMINANT OF THE DISPOSITION OF AROMATASE INHIBITORS IN EPITHELIAL CELLS OF INVASIVE DUCTAL CARCINOMA

Mostafizur Rahman, Sigurd F. Lax, Carrie H. Sutter, Quynh T. Tran, Gaylene L. Stevens, Gary L. Emmert, Jose Russo, Richard J. Santen, and Thomas R. Sutter

W. Harry Feinstone Center for Genomic Research, The University of Memphis, Memphis, TN 38152 (M.R., C.H.S., Q.T.T., G.L.S., T.R.S.); Department of Chemistry, The University of Memphis, Memphis, TN 38152 (M.R., G.L.E., T.R.S.); Department of Biology, The University of Memphis, Memphis, TN 38152 (M.R., C.H.S., Q.T.T., G.L.S., T.R.S.); Department of Pathology, General Hospital Graz West, Graz A-8020, Austria (S.F.L.); Fox Chase Cancer Center, Philadelphia, PA 19111 (J.R.); School of Medicine, University of Virginia, Charlottesville, Virginia 22908 (R.J.S.)

Running Title: Disposition of aromatase inhibitors by CYP1B1

Corresponding author:

Dr. Thomas R. Sutter, W. Harry Feinstone Center for Genomic Research, The University of Memphis, 201 Life Sciences Building, Memphis, TN 38152. Tel.: 901-678-8391; Fax: 901-678-2458; E-mail: tsutter@memphis.edu

The number of:

Text pages: 30

Figures: 5

Table: 1

References: 40

Number of Words: Abstract: 243

Introduction: 621

Discussion: 1199

Abbreviations used:

CYP1B1: cytochrome P4501B1; CYP19: cytochrome P45019 (aromatase); AI: aromatase inhibitor; E2: 17β-estradiol; 4-OHE2: 4-hydroxy estradiol; 2-OHE2: 2-hydroxy estradiol

Abstract

Cytochrome P4501B1 (CYP1B1) and CYP19 (aromatase) have been shown to be expressed in breast tumors. Both enzymes are efficient estrogen hydroxylases, indicating the potential for overlapping substrate and inhibitor specificity. We measured the inhibition properties of aromatse inhibitors (AIs) against CYP1B1-catalyzed hydroxylation of 17β-estradiol (E2) to determine whether CYP1B1 affects the disposition of AIs. In addition, we estimated the frequency of co-expression of these enzymes in breast tumor epithelium. Immunohistochemical analyses of CYP19 and CYP1B1 in a panel of 29 cases of invasive ductal carcinoma of the breast showed epithelial cell staining for CYP19 in 76% and for CYP1B1 in 97% of the samples. Statistical analysis showed no significant correlation (0.33) for positive expression of CYP19 and CYP1B1 ($P > 0.07$). CYP1B1 inhibition was determined for two steroidal inhibitors: formestane and exemestane, and five non-steroidal inhibitors: aminoglutethimide, fadrozole, anastrozole, letrozole, and vorozole. Of the seven compounds tested, only vorozole exhibited inhibition of CYP1B1 activity with IC_{50} values of 17 and 21 μM for 4-hydroxyestradiol (4-OHE2) and 2-hydroxyestradiol (2-OHE2), respectively. The estimated K_i values of vorozole for E2 4- and 2-hydroxylation were 7.26 and 6.84 μM, respectively. Spectrophotometric studies showed that vorozole was a type II inhibitor of CYP1B1. This study shows that with the exception of vorozole, the aromatase inhibitors are selective for CYP19 relative to CYP1B1. Thus, although both CYP19 and CYP1B1 are expressed in a high percentage of breast cancers, CYP1B1 is not a major determinant of the disposition of AIs.

Introduction

Cytochrome P45019 (CYP19, aromatase) catalyzes the formation of the phenolic A ring of estrogens, converting androstenedione to estrone and testosterone to estradiol (Johnston and Dowsett, 2003). CYP19 is found in glandular and nonglandular tissues including adrenal glands, ovaries, placenta, testes, adipose tissue, muscle, brain, normal breast, and breast cancer tissue. Important to this work, studies have shown that substantial levels of estrogens arise from aromatase activity in breast tissue (Miller, 1991; Bulun et al., 1993). CYP19 protein and activity have been detected in both the epithelial cells and surrounding stroma and adipose tissue of breast tumors (Esteban et al., 1992; Lu et al., 1996; Brodie et al., 1997; Oliveira et al., 2006; Miki et al., 2007). A recent study showed that while significant CYP19 immunoreactivity occurred in each of these cellular compartments of breast tumors, a significant positive correlation between biochemical activity and immunostaining was detected only for the epithelium (Sasano et al., 2005).

Aromatase inhibitors (AIs) are drugs that inhibit CYP19, preventing the formation of estrogens. The AIs are subdivided into steroidal (type I) and non-steroidal (type II) agents (Johnston and Dowsett, 2003; Miller, 2006). Type 1 agents are analogues of androgens that bind to CYP19 through either reversible or irreversible mechanisms, competing with the natural substrates. Type II inhibitors reversibly interact with the heme iron of cytochrome P450 (Miller, 2006). AIs are also categorized as first-, second-, and third-generation inhibitors based on their chronological order of clinical development (Johnston and Dowsett, 2003). AI therapy has been shown to be effective in the prevention of new and recurrent breast cancer in women previously treated for an estrogen receptor positive tumor. At present, third-generation AIs developed in the

early 1990s have been introduced into the treatment of estrogen receptor positive breast cancer in the metastatic, as well as the adjuvant settings (Joensuu et al., 2005).

Cytochrome P4501B1 (CYP1B1), an extrahepatic enzyme, is the third member of the CYP1 family and is the only known member of CYP1B subfamily (Sutter et al., 1994). It is expressed constitutively in many human tissues, including breast and ovary (Shimada et al., 1996; Jefcoate et al., 2000; Muskhelishvili et al., 2001). CYP1B1 is the most catalytically efficient 17β-estradiol (E2) hydroxylase, preferentially producing 4-hydroxy-E2 (Hayes et al., 1996). Furthermore, CYP1B1 can oxidize the catechol estrogens to the chemically reactive semiquinone and quinone intermediates that form DNA adducts that can initiate breast, prostate, and other types of cancer (Cavalieri et al., 2006). Increased E2 4-hydroxylase activity has been measured in human breast cancer compared to normal breast tissue (Liehr and Ricci, 1996), and increased expression of CYP1B1 protein has been shown to occur in several types of human cancers, including breast and ovary (McFadyen et al., 1999).

Expression of CYP19 (Esteban et al., 1992; Brodie et al., 1997; Oliveira et al., 2006; Miki et al., 2007; Sasano et al., 2005) and CYP1B1 (McFadyen et al., 1999) proteins have been detected in breast cancer independently by immunohistochemistry, indicating that these enzymes are major tumor forms of cytochrome P450 expressed in breast tumors. In addition, higher expression of CYP19 and CYP1B1 mRNAs has also been reported in breast cancer tissues compared to normal tissues (Singh et al., 2005), suggesting the importance of these two enzymes in the development and progression of breast cancer. Both CYP1B1 and CYP19 are efficient E2 hydroxylases (Jefcoate et al., 2000; Hayes et al., 1996; Liehr and Ricci, 1996; Singh et al., 2005; Aoyama et al., 1990), indicating the potential for overlapping substrate and inhibitor specificity. To determine whether CYP1B1 can affect the disposition of AIs, we measured the inhibition

DMD Fast Forward. Published on February 6, 2008 as DOI: 10.1124/dmd.107.018960
This article has not been copyedited and formatted. The final version may differ from this version.

properties of a series of AIs against CYP1B1-catalyzed hydroxylation of E2. In addition, the frequency of co-expression of these enzymes in breast tumor epithelium was estimated.

Materials and Methods

Materials. Human CYP19 and human CYP1B1 microsomes were purchased from BD Gentest (Woburn, MA, USA). The AIs obtained from multiple sources were kindly provided by Dr. William R. Miller (Western General Hospital, University of Edinburgh, Edinburgh, Scotland, UK). Formestane, letrozole, fadrozole, and aminoglutethimide were obtained from Novartis International AG (Basel, Switzerland). Exemestane was obtained from Pfizer (New York, USA). Anastrozole was obtained from AstraZeneca (Södertälje, Sweden), and vorozole from Jannsen (Beerse, Belgium). The other materials used in this study were described previously in detail (Rahman et al., 2006).

CYP19 protein expression and purification of hexahistidine – tagged proteins in *E. coli*. To generate fusion proteins, cDNA constructs were cloned into a vector engineered such that the expressed protein has an amino terminal hexahistidine peptide tag to allow purification by metal chelate affinity chromatography. For the human CYP19 expression construct (herein referred to as His_6-CYP19), a 730 bp Pst I – Kpn I fragment of the human aromatase cDNA [nucleotide positions, 395–1125] (Corbin et al., 1988) was subcloned into the Pst I – Kpn I site of vector pTrcHis C (Invitrogen, San Diego, CA, USA) and transformed into *E. coli* JM 109 cells. The cDNA orientation and reading frame were verified by DNA sequence analysis.

E. coli expression and purification followed our previously published methods (Walker et al., 1998). *E. coli*, transformed with His_6-CYP19 plasmid, were inoculated into 5 mL Terrific broth [1.2% (w/v) bacto-tryptone, 2.4% (w/v) bacto-yeast extract, 0.4% (v/v) glycerol, 17 mM KH_2PO_4, 72 mM K_2HPO_4] containing 100 μg/mL ampicillin (TB + Amp), and grown overnight at 37^{o}C at 200 rpm. The overnight culture (5 mL) was inoculated into 200 mL (His_6-CYP19) TB

DMD Fast Forward. Published on February 6, 2008 as DOI: 10.1124/dmd.107.018960
This article has not been copyedited and formatted. The final version may differ from this version.

+Amp and grown at 37^{o}C with vigorous shaking for about 2.5 h until the cells were in mid-log phase (A_{600} = 0.6-0.8). In order to induce protein expression, IPTG was added to a final concentration of 1 mM followed by incubation for 5 hours at 37^{o}C. A 0.5 ml cell sample was pelleted by centrifugation, resuspended, and boiled for 5 min in 100 µL SDS sample dilution buffer (50 mM Tris.Cl, pH 6.8, 1.5% 2-mercaptoethanol, 2% SDS, 0.1% bromophenol blue, 10% glycerol). Fifteen µL if this cell lysate were analyzed by sodium dodecyl sulfate-polyacrylamide gel electrophoresis (SDS-PAGE) to confirm induction of the 35 kDa His_6-CYP19 protein.

The induced *E. coli* culture (200 mL) was pelleted by centrifugation at 5000 x *g* for 10 min at 4^{o}C. The cells were resuspended and lysed in 6 M guanidinium hydrochloride, 100 mM sodium phosphate, 10 mM Tris.Cl, pH 8.0 and the hexahistidine-tagged protein was purified by affinity column chromatography with nickel-nitrilotriacetic acid (NTA)-agarose (Qiagen, Chatsworth, CA, USA). Elution of His_6-CYP19 from the NTA-agarose was achieved using a pH step-gradient (pH 8.0, pH 6.3, pH 4.5). Approximately 1 mg of affinity purified protein was then separated by SDS-PAGE using a 20-cm long 12% polyacrylamide gel and stained with 0.3 M copper-chloride ($CuCl_2$) for 5 min. The area of the gel containing the fusion protein was excised using a razor blade and destained by repeated washing in 0.25 M EDTA, 0.25 M Tris.Cl, pH 9.0. The protein was eluted from the gel slice by electroelution in 25 mM Tris base, 192 mM glycine, pH 8.8 containing 0.01% SDS, then dialyzed against 0.5 x phosphate buffered saline and frozen at -20^{o}C. The purity of the electroeluted protein was confirmed by coomassie stain of the protein analyzed by SDS-PAGE.

Generation of polyclonal antibodies. All animal procedures were carried out by Spring Valley Laboratories (Sykesville, MD, USA). A polyacrylamide gel slice containing 250 µg purified

DMD Fast Forward. Published on February 6, 2008 as DOI: 10.1124/dmd.107.018960
This article has not been copyedited and formatted. The final version may differ from this version.

fusion protein was minced and emulsified in complete Freund's adjuvant and used for primary subcutaneous immunization of New Zealand White male rabbits. Rabbits were boosted 2 and 4 weeks following the primary immunization with 200 μg purified protein, emulsified in incomplete Freund's adjuvant. Serum was prepared from blood taken 5 weeks following the primary immunization. The serum IgG was purified by protein A affinity purification [Pierce (Walker et al., 1998)].

Immunoblot analysis. Microsomal samples were solubilized in SDS sample dilution buffer and separated by denaturing SDS-PAGE. Separated proteins were transferred to nitrocellulose (Hybond ECL; Amersham Corporation, Arlington Heights, IL, USA) and incubated with primary antibody (anti-CYP19 at 5 μg/mL of purified IgG and anti-CYP1B1 (Walker et al., 1998) at 10 μg/mL) for 1 h at room temperature. Bound antibody was detected by incubation for 1 h with a horseradish peroxidase (HRP) linked secondary antibody [goat anti-rabbit IgG, 1:30,000 dilution (Promega Corporation, Madison, WI, USA)]. Bound secondary antibody was detected by an enhanced chemiluminescence (ECL) method according to the manufacturer's instructions (Pierce).

Immunohistochemical analysis. The purified serum IgG was used at a concentration of either 10 μg/mL (CYP19) or 10 μg/mL (CYP1B1). Non-specific staining was assessed using normal rabbit serum (Sigma) at a dilution of 1:5000. Paraffin-embedded human breast cancer samples including 29 cases of invasive ductal carcinoma (IDC), cases of cancer metastasis and samples of normal breast tissue adjacent to cancer tissue were obtained as tissue microarrays from Imgenex (IMH-36460 San Diego, CA, USA). Imgenex is the U.S. distributor for SuperBioChips (S.

Korea). Results for staining for ER, PR and P53 were provided by Imgenex with the tissue arrays. The source of antibodies for these proteins was DAKO (Glostrup, Denmark: ER, M7047; PR, A0098; P53, M7001). Both the breast and placental tissues were obtained as discarded tissue, without patient identifiers. The slides were deparaffinized in xylene (twice for 4 min) followed by washing in 100% ethanol (4 min), 95% ethanol (2 min), 80% ethanol (15 s) and distilled water. Immunohistochemistry was performed as described previously (Walker et al., 1998), using diaminobenzidine as the chromagen. The slides were washed with distilled water for 1 min and counterstained for 1 min with hematoxilin. The intensities of the immunreactivity were scored from 0-5 and the sample identifications were blinded from the pathologist (J.R.).

Statistical Analysis. Correlation between the epithelial cell expression of aromatase, CYP1B1, ER, PR, and p53 in IDC of the breast were determined using the Pearson chi-square test.

Inhibition kinetics assay using the microsomal fraction containing recombinant human CYP1B1. The recombinant human CYP1B1 protein was expressed in *S. cerevisiae* as described previously (Hayes et al., 1996). Specific CYP1B1 protein content was estimated and evaluated by measuring the enzymatic activity as previously described (Rahman et al., 2006). For the initial AI screen, the same preparation of CYP1B1 microsomes was used for the inhibition studies. The measured E2 4-hydroxylase activity was 1.23 nmol/min/nmol P450, consistent with the turnover number published in our previous studies (Hayes et al., 1996; Rahman et al., 2006). The inhibition kinetics of CYP1B1 was determined in a range expected to produce 30% to 90% inhibition. A fixed substrate concentration and varying inhibitor concentrations were used to determine the IC_{50} value at the point where 50% inhibition of the catalytic activity of the enzyme occurred. The E2 hydroxylation assay was performed with the addition of inhibitor and has been

previously described in detail (Rahman et al., 2006). Inhibition was calculated as percent of product formation compared to the corresponding control (enzyme-substrate reaction) without the inhibitors.

To determine the K_i value and type of inhibition from Dixon plots (Dixon, 1953), 10 pmol of human CYP1B1 was assayed in presence of three substrate concentrations: 1, 3, and 5 μM of E2, and five concentrations of vorozole: 0.0, 5.0, 10.0, 20.0, and 40.0 μM, respectively. The substrate concentrations were approximately equal to 0.5 x K_m, 2 x K_m, and 4 x K_m. The accurate values were 0.612 (0.5 x K_m), 2.45 (2 x K_m), and 4.89 (4 x K_m) μM. The concentration of vorozole was chosen and varied to give a wide range of percent inhibition based on our previously determined IC_{50} for this inhibitor. Linear regression analyses for each of the three substrate concentrations were plotted on a single graph of 1/rate versus inhibitor concentration. The rate of product formation was determined as pmol of product per minute in each reaction. The coordinates of intersection of regression lines in Dixon plots are $-K_i$ and $1/K_{cat}$. The K_i value is determined by averaging the results from individual intersections where the three regression lines did not intersect at a single point. Cornish-Bowden plot (S/V against i) was also constructed using the same data to model the type of inhibition (Cornish-Bowden, 1974).

Binding difference spectra of P4501B1 with vorozole. The binding of vorozole to CYP1B1 was monitored by difference spectroscopy (Schenkman et al., 1967). The P450 content in microsomes containing recombinant human CYP1B1 expressed in the yeast *S. cerevisia* was estimated to be 217.5 pmole/mg protein on the basis of reduced CO-difference spectra. The microsomal protein was suspended in 0.1 M KPO_4 buffer, pH 7.4. The diluted sample was transferred into both sample and reference cuvettes to give a protein concentration of 1 mg/mL

and the baselines of equal light absorbance were recorded using a Varian Cary 100 Bio UV-Visible spectrophotometer (Walnut Creek, CA, USA) between 350 and 500 nm at ambient temperature. After the baseline had been recorded, vorozole dissolved in DMSO was added to the sample cuvette in 2 μL aliquots and mixed gently with a pipette into the sample mixture. Vorozole was added to produce final concentrations of 5.0, 20.0, and 80.0 μM. An equal volume of carrier solvent was added to the reference cuvette. The sample was allowed to stand for 1 min and the difference spectra were determined (350-500 nm) after each addition and graphed with baseline and background correction.

Results

Expression of CYP19 protein in *E. coli* and production of polyclonal antibodies to CYP19. For the generation of polyclonal antibodies to CYP19, we expressed CYP19 as hexahistidine-tagged fusion proteins in *E. coli*. High expression of His_6-CYP19 was observed in protein extracts of induced *E. coli* cultures (Fig. 1A, lane 2). Metal chelate affinity purification yielded a 35 kDa CYP19 fusion protein and this was confirmed by SDS-PAGE (Fig. 1A, lanes 4-7). Immunoblot analyses using the anti His_6-CYP19 and anti His_6-CYP1B1 antibodies showed that these antibodies reacted with their corresponding proteins in microsomes prepared from insect cells expressing recombinant human proteins. A single immunoreactive band of 60 kDa was detected by the anti-CYP19 antibody. Similarly, a single immunoreactive band of 56 kDa was detected by the anti-CYP1B1 antibody (Fig. 1B). The specificity of the anti-CYP19 antibody was shown by immunoblot analysis of protein fractions prepared from human placental tissue (Fig. 1C) and immunohistochemistry of human placental tissue (Fig. 1D). Only a single band of approximately 60 kDa was detected in either microsomes (Fig. 1C, lane 1) or the post-mitochondrial supernatant (Fig. 1C, lane 2) prepared from two samples of human placenta. Immunohistochemistry demonstrated strong CYP19 staining in the syncytiotrophoblast of the placental villi (Fig. 1D, long arrow), with weaker staining in the cytotrophoblast and decidua (Fig. 1D). The strong staining of CYP19 in the syncytiotrophoblast of the placental villi has been reported for the characterization of other anti-CYP19 antibodies (Estaban et al., 1992). The sensitivity and specificity of the anti-CYP1B1 antibody has been reported previously (Walker et al., 1998; Kim et al., 2004). Representative immunohistochemical analyses of CYP19 and CYP1B1 expression in human breast invasive ductal carcinoma using the purified antibody are shown in Fig. 1C

DMD Fast Forward. Published on February 6, 2008 as DOI: 10.1124/dmd.107.018960
This article has not been copyedited and formatted. The final version may differ from this version.

Immunohistochemistry of breast cancer using anti-CYP19 and anti-CYP1B1 antibodies. In this study, we evaluated the immunohistochemical expression of CYP19 and CYP1B1 in epithelial cells of breast cancer primarily with IDC. The tissue array we evaluated had twenty-nine cases of IDC, as well as a small number of samples with metastatic carcinoma in lymph node (10 cases), infiltrating lobular carcinoma (2 cases), ductal carcinoma *in situ* (2 cases), singlet ring cell carcinoma (1 case), solid papillary carcinoma (1 case), and medullary carcinoma (1 case). Table 1 reports the epithelial cell expression of CYP19 and CYP1B1 in cases of IDC of the breast. The results show a high percentage of expression of both CYP19 and CYP1B1 in epithelium of IDC (22/29). Similar results were observed for metastatic carcinoma in lymph node (7/10), infiltrating lobular carcinoma (2/2), ductal carcinoma *in situ* (1/2), singlet ring cell carcinoma (1/1), solid papillary carcinoma (1/1), and medullary carcinoma (1/1), (data not shown). CYP19 was positive in 22 cases of IDC (75.86%). Other tissue compartments (data not shown) expressing CYP19 included the blood vessels (13.79% positive) and fibroblasts (34.48% positive). CYP1B1 was expressed at high frequency and was positive in 28 (96.55%) cases of IDC. Both CYP19 and CYP1B1 were positive in 22 (75.86%) cases. Estrogen receptor (ER), progesterone receptor (PR), and p53 were positive in 18 (62%), 11 (38%), and 12 (41%) cases, respectively. In addition to the IDC cases, we evaluated 10 samples of metastatic carcinoma in lymph node (LN) in epithelium for both CYP19 and CYP1B1 expression. We observed that CYP19 was positively expressed in LN in 8 (80%) cases, whereas CYP1B1 was positively expressed in 9 (90%) cases. Both CYP19 and CYP1B1 expression were positive in 70% cases (data not shown). In order to determine correlations between immunoreactivity of CYP19, CYP1B1, ER, PR, and p53, statistical analysis, using the Pearson chi-square test, was used. The correlation between the expression CYP19 and CYP1B1 was 0.33, and was not statistically

DMD Fast Forward. Published on February 6, 2008 as DOI: 10.1124/dmd.107.018960
This article has not been copyedited and formatted. The final version may differ from this version.

significant ($P > 0.07$). Furthermore, no statistically significant correlations were found between immunoreactivity for CYP19 and the estrogen receptor, the progesterone receptor, or p53 status. Also, no statistically significant correlations were found using the Fisher's exact test between CYP19 and CYP1B1 (data not shown).

The range of staining intensities of CYP19 and CYP1B1 were assigned scores 0-5 according to the intensity of the staining for the expression of each enzyme. The expression of CYP19 in breast epithelial cells ranged from 0-4, with a median value of 1; the expression of CYP1B1 ranged from 0-5, with a median value of 3. We also determined the p-value by Fisher's exact test using staining intensities with the histologic grading 0-5 and found no correlation between immunoreactivity of CYP19 and CYP1B1 (data not shown).

Inhibition of Human CYP1B1 Activity by AIs. To explore interactions of CYP1B1 as a potential effector of the disposition of the AIs, the inhibition properties of seven aromatase inhibitors were evaluated for CYP1B1-catalyzed hydroxylation of E2. The chemical structures of steroidal and non-steroidal aromatase inhibitors are shown in Fig. 2. The inhibition kinetics of steroidal (formestane and exemestane) and non-steroidal (aminoglutethimide, fadrozole, anastrozole, letrozole, and vorozole) AIs are presented in Fig. 3. None of the AIs tested were potent inhibitors of human CYP1B1 except vorozole. The IC_{50} values for formestane, exemestane, androstenedione, aminoglutethimide, fadrozole, anastrozole, and letrozole for human CYP1B1 E2 4- and 2-hydroxylation were found to be $\geq$100 μM. The IC_{50} values for vorozole for human CYP1B1 E2 4- and 2-hydroxylation were found to be 17 and 21 μM, respectively.

DMD Fast Forward. Published on February 6, 2008 as DOI: 10.1124/dmd.107.018960
This article has not been copyedited and formatted. The final version may differ from this version.

Because of the observed lower IC_{50} values for vorozole compared to other AIs investigated, we determined the K_i value of vorozole. The Dixon plot was used to determine the dissociation constant, K_i, for the binding of inhibitor to enzyme and also to demonstrate the mechanism of inhibition of vorozole (Dixon, 1953). Figure 4A and 4B show Dixon plots for the inhibition of CYP1B1 by vorozole. The intersection of the regression lines in the upper left quadrant of a Dixon plot indicates competitive inhibition. The K_i values of vorozole for E2 4- and 2-hydroxylation by CYP1B1 were found to be 7.26 and 6.84 μM, respectively. It has been reported that for competitive inhibition kinetics, the K_i does not equal to IC_{50} (Cheng and Prusoff, 1973). We also observed here that IC_{50} and K_i values of vorozole for E2 4- and 2-hydroxylation are different. To provide further unambiguous indication of the type of inhibition, a Cornish-Bowden plot was drawn using the same data (Cornish-Bowden, 1974). We plotted substrate concentration over rate (s/v) versus inhibitor concentration (*i*), at 1 and 5 μM substrate concentrations (Figs. 4C and 4D). Linear regression analyses for each of the two substrate concentrations were plotted on a single graph, which is similar to the Dixon plot, but complementary to it. It has been suggested that for competitive inhibition, if such lines are drawn, there is no intersection i.e. the lines are parallel in the plot of s/v against inhibitor concentration. Figure 4C and 4D show similar parallel lines, which further indicate the competitive type of inhibition for vorozole.

Binding of vorozole to CYP1B1 by difference spectroscopy. Addition of vorozole to the microsomal CYP1B1 protein resulted in the formation of a type II binding spectrum (Fig. 5). Addition of varying concentrations of vorozole resulted in a progressive spectral change. The spectral change was characterized by the appearance of an absorption peak at about 422 nm, a trough at about 390 nm, and an isosbestic point at about 410 nm.

Discussion

Here, we report the production and characterization of a specific antibody raised against hexahistidine-tagged fusion protein of CYP19 that was produced and purified from *E. coli*. The expressions of CYP19 and CYP1B1 in cases of breast cancer were studied by immunohistochemical analysis. These analyses showed that a high percentage (76%) of the cases of IDC of the breast expressed both enzymes in the ductal epithelium. However, statistical analysis showed no significant correlation between the immunohistochemical expression of CYP19 and CYP1B1; the observed correlation was 0.33 ($p>0.07$). Other characteristics of the tumor such as ER, PR, and p53 status did not show any statistically significant correlation with tumor aromatase. It should be noted that the number of cases of IDC evaluated in this study was small (n=29). A recent paper in a population based study (n=698) on hormonal markers in breast cancer identified a significant correlation ($p<0.01$, Pearson correlation coefficient = 0.14) between CYP19 and CYP1B1 (Yang et al., 2007). We believe that the likely reason for the difference in results between this study and ours is sample size, with the larger study (Yang et al., 2007) having greater power to detect this correlation. In another study (Esteban et al., 1992), a significant ($P = 0.04$), but inverse correlation between CYP19 and ER immunoreactivity was reported, indicating a likelihood of detecting CYP19 in ER-negative tumors. A significant correlation between the expression of cyclooxygenase-2 and CYP19 in IDC and ductal carcinoma *in situ* from the same breast has also been reported (Oliveira et al., 2006). This group reported that 70% of the samples stained positive for CYP19 enzyme expression. In a recent study, two new CYP19 monoclonal antibodies were described and validated in an analysis of 43 cases of IDC (Sasano et al., 2005). Importantly, this latter study (Sasano et al., 2005) showed that

there was a significant positive correlation between biochemical activity and CYP19 immunopositivity only in malignant epithelium.

CYP1B1 protein is overexpressed in malignant tumors of the breast (McFadyen et al., 1999). Interestingly, the elevated expression of CYP1B1 protein in breast cancer tissues has recently been shown to be regulated by microRNA (miRNA) expression (Tsuchiya et al., 2006). The researchers found that there was a significant inverse association between the expression levels of a specific miRNA (miR-27b) and CYP1B1 protein. It has been suggested that decreased expression of miR-27b would be one of the causes of the high expression of CYP1B1 protein in cancerous tissues. To our knowledge, the potential influence of miRNAs on the expression of CYP19 protein in tumor tissues has not been investigated.

As an approach to evaluate CYP1B1 as a potential determinant of the disposition of AIs, we determined the inhibition properties of a series of AIs against CYP1B1-catalyzed hydroxylation of E2. Instead of measuring metabolites of each compound, we screened the AIs for inhibition of CYP1B1, as competitive inhibitors may also be enzyme substrates. Of the seven compounds tested, only vorozole, a triazole derivative, exhibited potent inhibition of human CYP1B1 activity. The other AIs studied, formestane, exemestane, aminoglutethimide, fadrozole, anastrozole, and letrozole, showed only weak inhibition of the catalytic activity of CYP1B1. The Dixon and Cornish-Bowden plots indicate that there is a competitive part in the inhibition of the human CYP1B1 enzyme by vorozole. Previously, this compound has been reported as a competitive inhibitor of aromatase (Montellano, 1995). Although vorozole inhibits human CYP1B1, this compound is over a thousands-fold more active for aromatase inhibition (Wouters et al., 1994). It is unclear why other non-steroidal inhibitors were not found to be as effective as vorozole in decreasing the catalytic activity of CYP1B1. These differences of action on CYP1B1

by non-steroidal inhibitors may be due to the differences in their chemical structures. While the inhibitory activities of AIs against human CYP1B1 have not been previously studied, the effect of tamoxifen, a non-estradiol antiestrogen and a chemopreventive agent widely used for breast cancer treatment, was tested against human CYP1B1 as a possible inhibitor. However, the results of these studies were inconsistent (Rochat et al., 2001; Sridar et al., 2002). Rochat et al. (2001) have reported that tamoxifen, reversibly inhibits CYP1B1, and is a noncompetitive inhibitor. However, in another independent study, Sridar et al. (2002) mentioned that tamoxifen had no effect on the activities of CYP1B1.

The binding of vorozole to human CYP1B1 resulted in type II spectra (Fig. 5), which indicates that this compound is likely associated with ligation of the heme iron (Miller, 2006). It has been reported that this type of binding arises from the nitrogen interaction with the iron atom. The chemical structures of type II compounds usually possess atoms with freely accessible non-bonding electrons, such as nitrogen lone pair or aromatic and aliphatic amines (Schenkman et al., 1967; Miller, 2006). It is to be noted that vorozole, a non-steroidal type II inhibitor, like other non-steroidal compounds, has basic nitrogen atoms that allows the inhibitors to interact reversibly with the heme prosthetic group, a common feature of all cytochrome P450 enzymes (Johnston and Dowsett, 2003). Thus, vorozole is unlikely to be a substrate for CYP1B1. Preliminary studies with microsomal incubation of CYP1B1 with vorozole indicate no metabolic products as determined by HPLC with UV/Vis (data not shown).

AIs have been proposed for the prevention of breast cancer. In adjuvant therapy trials comparing tamoxifen with AIs, the reduction of contralateral breast cancer is 50% greater with the AI than with tamoxifen in separate trials (Kudachadkar and O'Regan, 2005). It has been postulated that the greater efficacy of the AIs is because of the reduction of estrogen levels and

therefore their genotoxic metabolites. Vorozole reduced plasma levels of E2 in premenopausal women to ~36% after 8 hour of intake (Wouters et al., 1989). It was also a more effective estrogen suppressant resulting in 30% more suppression of serum E2 levels in postmenopausal women than formestane, a steroidal inhibitor (Dowsett et al., 1999). However, vorozole has not been approved for use by the United States Food and Drug Administration (FDA), although its clinical activity was similar to anastrazole and letrozole in Phase III trials (Hamilton and Piccart, 1999). It has been reported that at clinically administered doses, the plasma half-lives of anastrozole (1 mg/day), letrozole (2.5 mg/day), and exemestane (25 mg/day) are 41-48 h, 2-4 days, and 27 h, respectively (Buzdar, 2003). There are some differences in the degree of plasma estradiol suppression among the third-generation AIs. The three aromatase inhibitors anastrozole, letrozole, and exemestane, that are currently approved by the FDA for use in breast cancer treatment, decrease estradiol by 84.9%, 87.8%, and 92.2%, respectively (Osborne and Tripathy, 2005). The third-generation AIs are well tolerated and suppress endogenous estrogen levels in postmenopausal women, but estrogen deficiency is one of the most important factors for the pathogenesis of osteoporosis. Osteoporotic fractures and greater bone mineral loss are typically more associated with AIs (Osborne and Tripathy, 2005, Lester and Coleman, 2005). Based on the results of this study, it is indicated that with the exception of vorozole, the AIs are specific for aromatase relative to CYP1B1, a cytochrome P450 widely expressed in breast tissue and responsible for estrogen metabolism. Overall, the results of this study indicate that CYP1B1 is not a major determinant of the disposition of AIs.

Acknowledgments

We thank Dr. William R. Miller for providing the aromatase inhibitors and his valuable comments in the preparation of the manuscript. We also thank Ms. Kimberly Reid and Ms. Monali Master for assistance with microsomes preparation, and Ms. Jennifer Tzefakes and Ms. Lou Boykins of the Integrated Microscopy Center for technical support with immunohistochemistry.

References

Aoyama T, Korzekwa K, Nagata K, Gillette J, Gelboin HV, and Gonzalez FJ (1990) Estradiol metabolism by complementary deoxyribonucleic acid-expressed human cytochrome P450s. *Endocrinology* **126:**3101-3106.

Brodie A, Lu Q, and Nakamura J (1997) Aromatase in the normal breast and breast cancer. *J Steroid Biochem Mol Biol* **61:**281-286.

Bulun SE, Price TM, Aitken J, Mahendroo MS, and Simpson ER (1993) A link between breast cancer and local estrogen biosynthesis suggested by quantification of breast adipose tissue aromatase cytochrome P450 transcripts using competitive polymerase chain

Cavalieri E, Chakravarti D, Guttenplan J, Hart E, Ingle J, Jankowiak R, Muti P, Rogan E, Russo J, Santen R, and Sutter T (2006) Catechol estrogen quinones as initiators of breast and other human cancers: implications for biomarkers of susceptibility and cancer prevention. *Biochim Biophys Acta* **1766:**63-78.

Cheng YC and Prusoff WH (1973) Relationship between the inhibition constant (K_I) and the concentration of inhibitor which causes 50 per cent inhibition (I_{50}) of an enzymatic reaction. *Biochem Pharmacol* **22:**3099-3108.

Corbin CJ, Graham-Lorence S, McPhaul M, Mason JI, Mendelson CR, and Simpson ER (1988) Isolation of a full-length cDNA insert encoding human aromatase system cytochrome P-450 and its expression in nonsteroidogenic cells. *Proc Natl Acad Sci USA* **85:**8948-8952.

Cornish-Bowden A (1974) A simple graphical method for determining the inhibition constants of mixed, uncompetitive and non-competitive inhibitors. *Biochem J* **137:**143-144.

Dixon M (1953) The determination of enzyme inhibitor constants. *Biochem J* **55:**170-171.

Dowsett M, Doody D, Miall S, Howes A, English J, and Coombes RC (1999) Vorozole results in greater oestrogen suppression than formestane in postmenopausal women and when added to goserelin in premenopausal women with advanced breast cancer. *Breast Cancer Res Treat* **56:**25-34.

Esteban JM, Warsi Z, Haniu M, Hall P, Shively JE, and Chen S (1992) Detection of intratumoral aromatase in breast carcinomas. An immunohistochemical study with clinicopathologic correlation. *Am J Pathol* **140:**337-343.

Hamilton A and Piccart M (1999) The third-generation non-steroidal aromatase inhibitors: a review of their clinical benefits in the second-line hormonal treatment of advanced breast cancer. *Ann Oncol* **10:**377-384.

Hayes CL, Spink DC, Spink BC, Cao JQ, Walker NJ, and Sutter TR (1996) 17β-Estradiol hydroxylation catalyzed by human cytochrome P450 1B1. *Proc Natl Acad Sci USA* **93:**9776-9781.

Jefcoate CR, Liehr JG, Santen RJ, Sutter TR, Yager JD, Yue W, Santner SJ, Tekmal R, Demers L, Pauley R, Naftolin F, Mor G, and Berstein L (2000) Tissue-specific synthesis and oxidative metabolism of estrogens. *J Natl Cancer Inst Monogr* **27:**95-112.

Joensuu H, Ejlertsen B, Lonning PE, and Rutqvist LE (2005) Aromatase inhibitors in the treatment of early and advanced breast cancer. *Acta Oncol* **44:**23-31.

Johnston SR and Dowsett M (2003) Aromatase inhibitors for breast cancer: lessons from the laboratory. *Nat Rev Cancer* **3:**821-831.

Kim JH, Sherman, ME, Curriero FC, Guengerich FP, Strickland PT, and Sutter TR (2004) Expression of cytochromes P450 1A1 and 1B1 in human lung from smokers, non-smokers, and ex-smokers. *Toxicol. Appl. Pharmacol.* **199:** 210-219.

Kudachadkar R and O'Regan RM (2005) Aromatase inhibitors as adjuvant therapy for postmenopausal patients with early stage breast cancer. *CA Cancer J Clin* **55:**145-163.

Liehr JG and Ricci MJ (1996) 4-Hydroxylation of estrogens as marker of human mammary tumors. *Proc Natl Acad Sci USA* **93:**3294-3296.

Lu Q, Nakmura J, Savinov A, Yue W, Weisz J, Dabbs DJ, Wolz G, and Brodie A (1996) Expression of aromatase protein and messenger ribonucleic acid in tumor epithelial cells and evidence of functional significance of locally produced estrogen in human breast cancers. *Endocrinology* **13**7:3061-3068.

McFadyen MC, Breeman S, Payne S, Stirk C, Miller ID, Melvin WT, and Murray GI (1999) Immunohistochemical localization of cytochrome P450 CYP1B1 in breast cancer with monoclonal antibodies specific for CYP1B1. *J Histochem Cytochem* **47:**1457-1464.

Miki Y, Suzuki T, Tazawa C, Yamaguchi Y, Kitada K, Honma S, Moriya T, Hirakawa H, Evans DB, Hayashi S, Ohuchi N, and Sasano H (2007) Aromatase localization in human breast cancer tissues: possible interactions between intratumoral stromal and parenchymal cells. *Cancer Res* **67:**3945-3954.

Miller WR (2006) Aromatase and the breast: regulation and clinical aspects. *Maturitas* **54:**335-341.

Miller WR (1991) Aromatase activity in the breast tissue. *J Steroid Biochem Mol Biol* **39:**783-790.

Montellano PRO (1995) Cytochrome P450 Structure, Mechanism, and Biochemistry. Second edition, Plenum Press, New York.

Muskhelishvili L, Thompson PA, Kusewitt DF, Wang C, and Kadlubar FF (2001) In situ hybridization and immunohistochemical analysis of cytochrome P450 1B1 expression in human normal tissues. *J Histochem Cytochem* **49:**229-236.

Oliveira VM, Piato S, and Silva MA (2006) Correlation of cyclooxygenase-2 and aromatase immunohistochemical expression in invasive ductal carcinoma, ductal carcinoma in situ, and adjacent normal epithelium. *Breast Cancer Res Treat* **95:**235-241.

Osborne C and Tripathy D (2005) Aromatase inhibitors: rationale and use in breast cancer. *Annu Rev Med* **56:**103-116.

Rahman M, Sutter CH, Emmert GL, and Sutter TR (2006) Regioselective 2-hydroxylation of 17β-estradiol by rat cytochrome P4501B1. *Toxicol Appl Pharmacol* **216:**469-478.

Rochat B, Morsman JM, Murray GI, Figg WD, and Mcleod HL (2001) Human CYP1B1 and anticancer agent metabolism: mechanism for tumor-specific drug inactivation? *J Pharmacol Exp Ther* **296:**537-541.

Sasano H, Anderson TJ, Silverberg SG, Santen RJ, Conway M, Edwards DP, Krause A, Bhatnagar AS, Evans DB, and Miller WR (2005) The validation of new aromatase monoclonal antibodies for immunohistochemistry-a correlation with biochemical activities in 46 cases of breast cancer. *J Steroid Biochem Mol Biol* **95:**35-39.

Schenkman JB, Remmer H, and Estabrook RW (1967) Spectral studies of drug interaction with hepatic microsomal cytochrome. *Mol Pharmacol* **3:**113-123.

Shimada T, Hayes CL, Yamazaki H, Amin S, Hecht SS, Guengerich FP, and Sutter TR (1996) Activation of chemically diverse procarcinogens by human cytochrome P-4501B1. *Cancer Res* **56:**2979-2984.

Singh S, Chakravarti D, Edney JA, Hollins RR, Johnson PJ, West WW, Higginbotham SM, Cavalieri EL, and Rogan EG (2005) Relative imbalances in the expression of estrogen-metabolizing enzymes in the breast tissue of women with breast carcinoma. *Oncol Rep* **14:**1091-1096.

Sridar C, Kent UM, Notley LM, Gillam EMJ, and Hollenberg PF (2002) Effect of tamoxifen on the enzymatic activity of human cytochrome CYP2B6. *J Pharmacol Exp Ther* **301:**945-952.

Sutter TR, Tang YM, Hayes CL, Wo YY, Jabs EW, Li X, Yin H, Cody CW, and Greenlee WF (1994) Complete cDNA sequence of a human dioxin-inducible mRNA identifies a new gene subfamily of cytochrome P450 that maps to chromosome 2. *J Biol Chem* **69:**13092-13099.

Tsuchiya Y, Nakajima M, Takagi S, Taniya T, and Yokoi T (2006) MicroRNA regulates the expression of human cytochrome P4501B1. *Cancer Res* **66:**9090-9098

Walker NJ, Crofts FG, Li Y, Lax SF, Hayes CL, Strickland PT, Lucier GW, and Sutter TR (1998) Induction and localization of cytochrome P450 1B1 (CYP1B1) protein in the livers of TCDD-treated rats: detection using polyclonal antibodies raised to histidine-tagged fusion proteins produced and purified from bacteria. *Carcinogenesis* **19:**395-402.

Wouters W, Coster RD, Tuman RW, Bowden CR, Bruynseels J, Vanderpas H, Van Rooy P, Amery WK, and Janssen PA (1989) Aromatase inhibition by R 76713: Experimental and clinical pharmacology. *J Steroid Biochem* **34:**427-430.

Wouters W, Snoeck E, and Coster RD (1994) Vorozole, a specific non-steroidal aromatase inhibitors. *Breast Cancer Res Treat* **30:**89-94.

Yang, XR, Pfeiffer RM, Garcia-Closas M, Rimm DL, Lissowska J, Brinton LA, Peplonska B, Hewitt SM, Cartun R, Mandich D, Sasano H, Evans DB, Sutter TR, and Sherman ME (2007) Hormonal markers in breast cancer: co-expression, relationship with pathologic characteristics and risk factor associations in a population-based study. *Cancer Res* **67:**10608-10617.

Footnotes

This work was supported by grants from the NIH, ES 08148, and the DOD, DAMD 17-03-1-0229, and the W. Harry Feinstone Center for Genomic Research.

Figure Legends

Figure 1. Expression of CYP19 and CYP1B1 in human breast invasive ductal carcinoma. **A,** expression and purification of His_6-CYP19 fusion protein from *E. coli*. Protein samples were fractionated on a 12% SDS-PAGE and stained with Coomassie blue. Lane 1, molecular wt standards (kDa); Lane 2, induced *E. coli* cultures (15 μL cell lysate was loaded as described in Materials and Methods; Lane 3, uninduced *E. coli* cultures; Lane 4-7, fractions of fusion protein purified by nickel-chelate affinity chromatography. **B,** immunoblots of CYP19 and CYP1B1. Lane 1 & 3, 1 pmole of recombinant CYP19 microsomes from BD Gentest (Woburn, MA, USA); Lane 2 & 4, 1 pmole of recombinant CYP1B1 microsomes from BD Gentest. **C,** immunoblot of CYP19 in fractions of human placental tissue (1:2000 dilution of anti-CYP19 antibody). Lane 1, 100 μg of microsomal protein from placenta B; lane 2, 100 μg of post-mitochondrial supernatant from placenta C. **D,** immunohistochemical analysis of CYP19 expression in placental tissue. CYP19 is strongly expressed in the syncytiotrophoblast of the placental villi (long arrow) and weakly expressed in the cytotrophoblast (short arrow) and decidua (asterisk). Photograph is at a magnification of X 200. **E,** immunohistochemical analyses of CYP1B1 (left) and CYP19 (right) expression in human breast cancer (invasive ductal carcinoma) samples. The upper panels are immunostained sample from the same individual in the same region. The lower panels are immunostained sample from another individual in the same region. Photographs are at a magnification of X 400.

Figure 2. Chemical structures of seven aromatase inhibitors. Steroidal inhibitors: formestane and exemestane; non-steroidal inhibitors: aminogultethimide, fadrozole, anastrozole, letrozole, and vorozole.

Figure 3. Inhibition of human CYP1B1 by aromatase inhibitors. Microsomes containing 10 pmol of CYP1B1 were incubated with 3 μM of E2 and 0.0, 1.0, 10.0, and 100 μM of each aromatase inhibitors in a single determination. Reactions were run for 15 min at 37^{o}C and rates of 4-OHE2 (hatched bar) and 2-OHE2 (open bar) formation were determined as described in 'Materials and Methods'.

Figure 4. Determination of K_i values and type of inhibition. **A & B.** Dixon plots for the inhibition of human CYP1B1 by vorozole. The inhibitor was tested in single determination at five concentrations in the presence of 1, 3, and 5 μM of E2. The reactions contained 10 pmol of CYP1B1 and were run for 15 min at 37^{o}C. **A,** human CYP1B1 (4-OHE2); **B,** human CYP1B1 (2-OHE2). ▼, 1 μM; ▲, 3 μM; ■, 5 μM E2. **C & D.** Cornish-Bowden plots for the inhibition of human CYP1B1 by vorozole. The plots were constructed using the same data. **C,** human CYP1B1 (4-OHE2); **D,** human CYP1B1 (2-OHE2). ▲, 1 μM; ■, 5 μM E2.

Figure 5. Binding spectra of vorozole to human CYP1B1 expressed in yeast. Microsomal protein (1 mg/ml) was suspended in 0.1 M KPO_4 buffer (pH 7.4) and placed in two cuvettes. The difference spectrum was obtained by adding vorozole to a final concentration of 5.0, 20.0, and 80.0 μM dissolved in DMSO in the sample cuvette, and an equal volume of carrier solvent added to the reference cuvette.

DMD Fast Forward. Published on February 6, 2008 as DOI: 10.1124/dmd.107.018960
This article has not been copyedited and formatted. The final version may differ from this version.

Table 1: Summary of statistical analysis of epithelial cell expression of CYP19 and CYP1B1 in invasive ductal carcinoma of the breast

		Aromatase negative	Aromatase positive	Total	P-value*	Correlation coefficient
CYP1B1						
	negative	1	0	1	0.0712	0.33503
	positive	6	22	28		
ER						
	negative	3	8	11	0.7578	0.05727
	positive	4	14	18		
PR						
	negative	4	14	18	0.7578	-0.05727
	positive	3	8	11		
p53						
	negative	4	13	17	0.9274	-0.01693
	positive	3	9	12		

* Analysis by the Pearson chi-square test

DMD Fast Forward. Published on February 6, 2008 as DOI: 10.1124/dmd.107.018960
This article has not been copyedited and formatted. The final version may differ from this version.

Figure 1

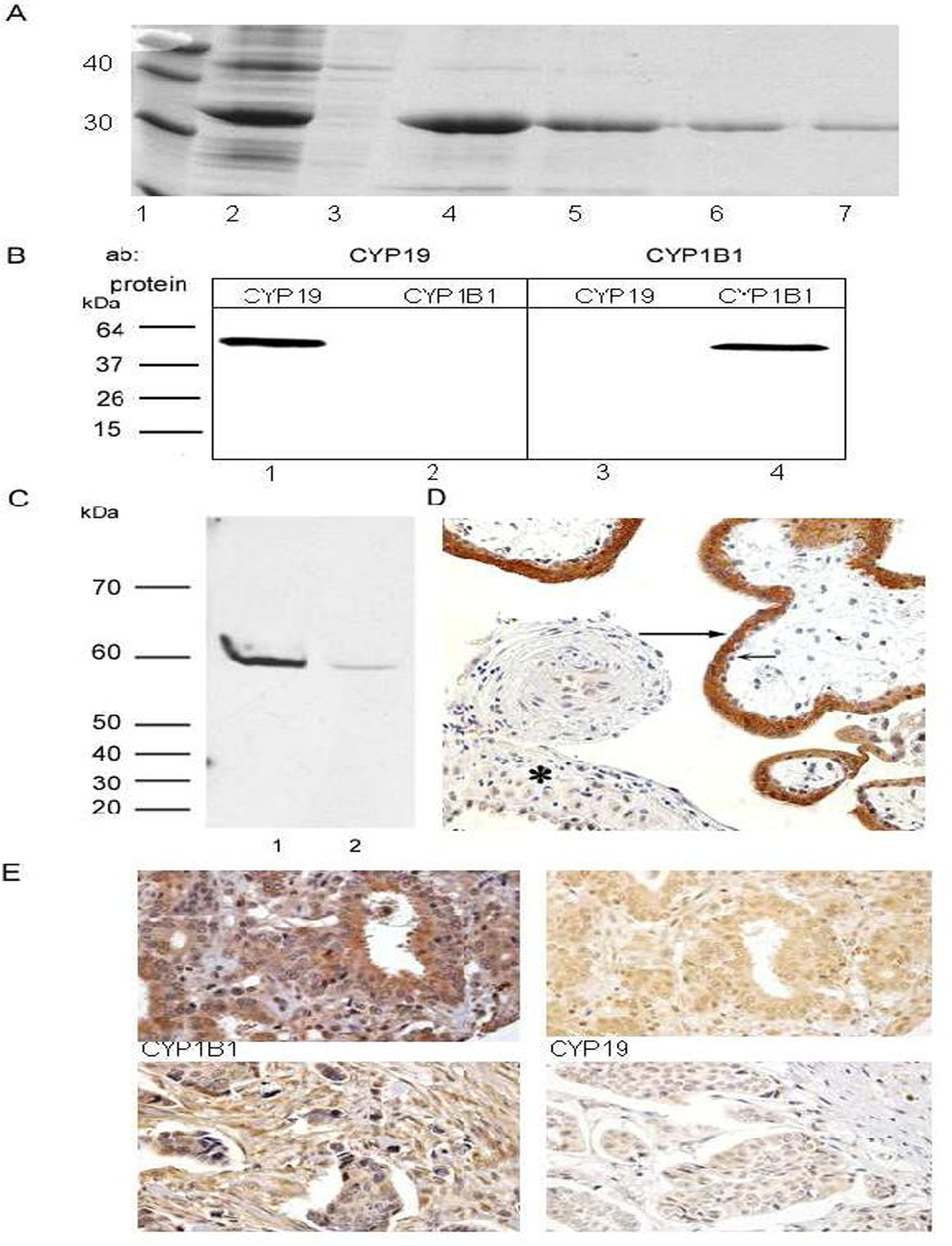

DMD Fast Forward. Published on February 6, 2008 as DOI: 10.1124/dmd.107.018960
This article has not been copyedited and formatted. The final version may differ from this version.

Figure 2

Steroidal inhibitors

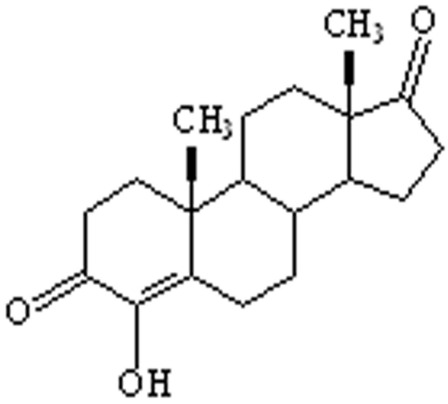

Formestane
(4-hydroxyandrostenedione)

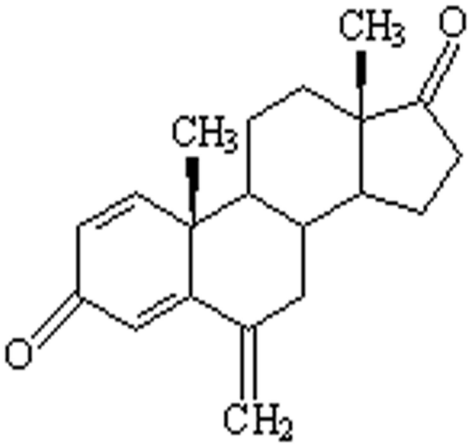

Exemestane

Non-steroidal inhibitors

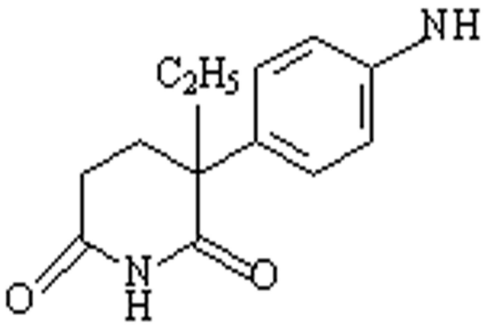

Aminoglutethimide

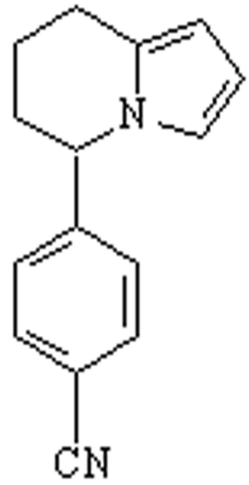

Fadrozole

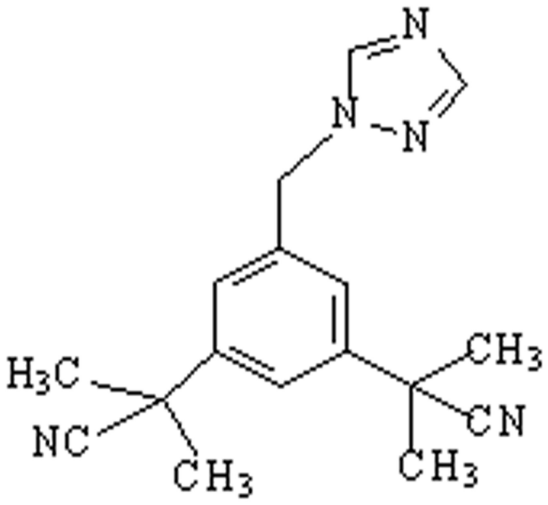

Anastrozole

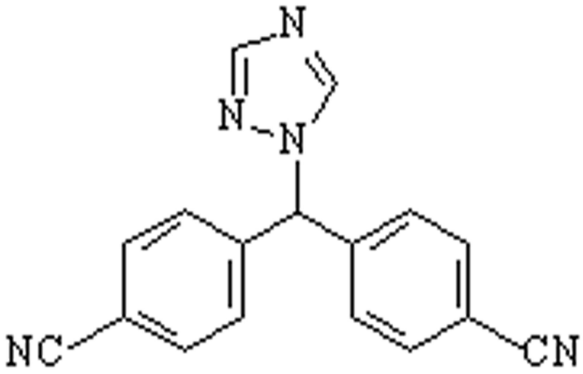

Letrozole

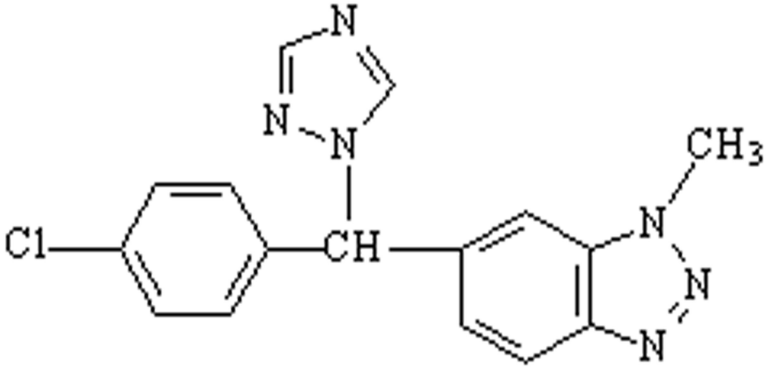

Vorozole

DMD Fast Forward. Published on February 6, 2008 as DOI: 10.1124/dmd.107.018960
This article has not been copyedited and formatted. The final version may differ from this version.

Figure 3

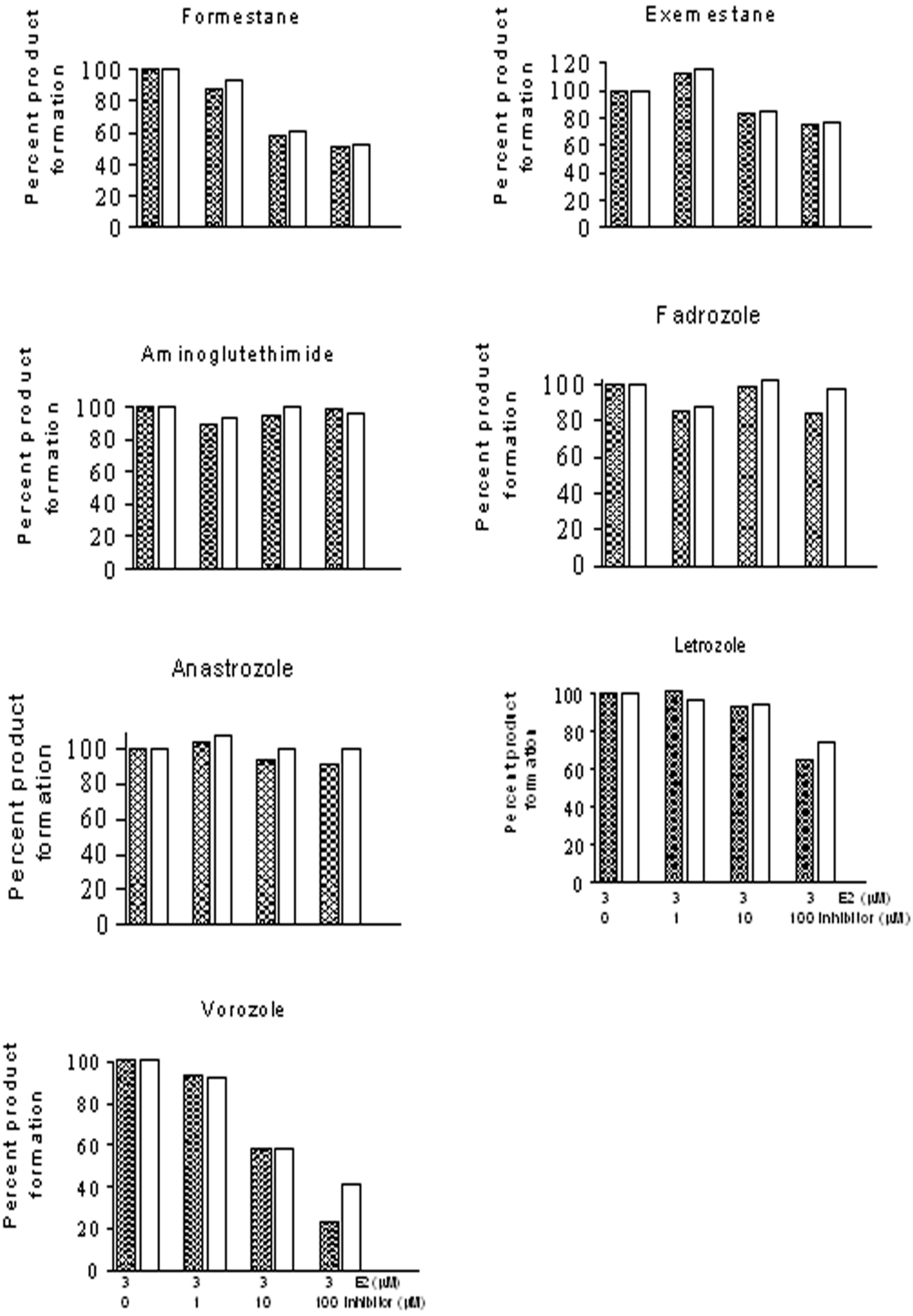

DMD Fast Forward. Published on February 6, 2008 as DOI: 10.1124/dmd.107.018960
This article has not been copyedited and formatted. The final version may differ from this version.

Figure 4

A

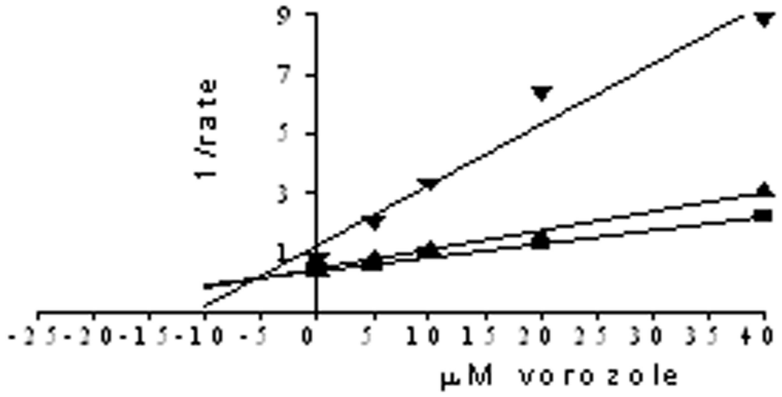

B

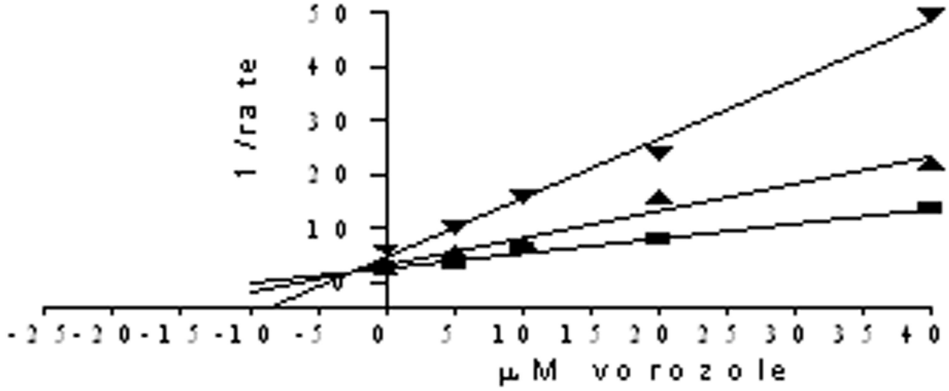

C

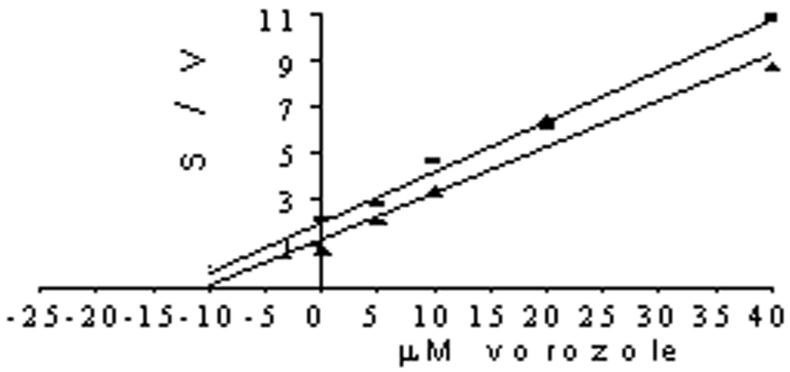

D

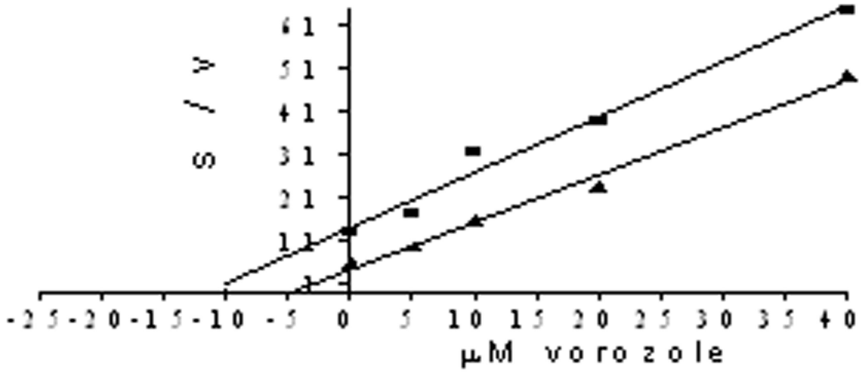

DMD Fast Forward. Published on February 6, 2008 as DOI: 10.1124/dmd.107.018960
This article has not been copyedited and formatted. The final version may differ from this version.

Figure 5